Published in final edited form as:
ACS Chem Biol. 2013 September 20; 8(9): 1955–1963. doi:10.1021/cb400274z.

Sulfopeptide probes of the CXCR4/CXCL12 interface reveal oligomer-specific contacts and chemokine allostery

Joshua J. Ziarek[1,*], **Anthony E. Getschman**[2,*], **Stephen J. Butler**[3], **Deni Taleski**[3], **Bryan Stephens**[4], **Irina Kufareva**[4], **Tracy M. Handel**[4], **Richard J. Payne**[3], and **Brian F. Volkman**[2,†]

[1]Department of Biological Chemistry and Molecular Pharmacology, Harvard Medical School, Boston, Massachusetts, USA.

[2]Department of Biochemistry, Medical College of Wisconsin, Milwaukee, Wisconsin, USA.

[3]School of Chemistry, The University of Sydney, NSW 2006, Australia.

[4]Skaggs School of Pharmacy and Pharmaceutical Science, University of California, San Diego, La Jolla, California, USA.

Abstract

Tyrosine sulfation is a post-translational modification that enhances protein-protein interactions and may identify druggable sites in the extracellular space. The G protein-coupled receptor CXCR4 is a prototypical example with three potential sulfation sites at positions 7, 12 and 21. Each receptor sulfotyrosine participates in specific contacts with its chemokine ligand in the structure of a soluble, dimeric CXCL12:CXCR4(1–38) complex, but their relative importance for CXCR4 binding and activation by the monomeric chemokine remains undefined. NMR titrations with short sulfopeptides showed that the tyrosine motifs of CXCR4 varied widely in their contributions to CXCL12 binding affinity and site specificity. Whereas the Tyr21 sulfopeptide bound the same site as in previously solved structures, the Tyr7 and Tyr12 sulfopeptides interacted nonspecifically. Surprisingly, the unsulfated Tyr7 peptide occupied a hydrophobic site on the CXCL12 monomer that is inaccessible in the CXCL12 dimer. Functional analysis of CXCR4 mutants validated the relative importance of individual CXCR4 sulfotyrosine modifications (Tyr21 > Tyr12 > Tyr7) for CXCL12 binding and receptor activation. Biophysical measurements also revealed a cooperative relationship between sulfopeptide binding at the Tyr21 site and CXCL12 dimerization, the first example of allosteric behavior in a chemokine. Future ligands that occupy the sTyr21 recognition site may act as both competitive inhibitors of receptor binding and allosteric modulators of chemokine function. Together, our data suggests that sulfation does not ubiquitously enhance complex affinity and that distinct patterns of tyrosine sulfation could encode oligomer selectivity – implying another layer of regulation for chemokine signaling.

INTRODUCTION

Chemokines are small soluble proteins that stimulate chemotactic cell migration via activation of a G protein-coupled receptor (GPCR). In addition to their vital roles in inflammation, wound healing, and stem cell homing, chemokines also contribute to many pathologies including autoimmune diseases and cancer. Interactions of the chemokine CXCL12 (stromal cell-derived factor-1/SDF-1) and its receptor CXCR4 are particularly well studied because of their participation in neurogenesis (1, 2), cardiogenesis (3), angiogenesis

†Corresponding author, bvolkman@mcw.edu.
*Equal contributors

Supporting Information Available: This material is available free of charge via the Internet at http://pubs.acs.org.

(4), myocardial infarction/reperfusion injury (5–7), HIV infection (8), and numerous carcinomas and sarcomas (as reviewed in (9)).

Chemokine receptor recognition and activation occurs via a two-step, two-site process (10, 11). First, the CXCR4 extracellular N-terminus binds to CXCL12 (site 1). The N-terminus of CXCL12 then recognizes the receptor transmembrane domain and activates signaling (site 2). Farzan and colleagues were the first to investigate the effect of post-translational modifications in the site 1 interaction (12). In addition to one site of *O*-linked glycosylation, CXCR4 possesses three tyrosine residues (Tyr7, Tyr12, and Tyr21) in the N-terminus capable of being *O*-sulfated in the Golgi apparatus. Mutational studies suggested that sulfation of Tyr21 enhances the binding of wild type CXCL12 ($CXCL12_{WT}$), but the level of sulfation at each tyrosine and their relative contributions to chemokine recognition were not quantified. Consistent with studies of the full-length CXCR4 receptor expressed in cells, sequential sulfation of a peptide comprising residues 1–38 ($CXCR4_{1–38}$) enhanced the affinity for CXCL12 (13). Full-length chemokine receptors CCR2b, CCR5, CCR8, CXCR3, and CX_3CR1 have since been shown to also exhibit increased ligand binding affinity upon tyrosine sulfation; replacement of tyrosines with phenylalanine residues resulted in 10 to 200-fold decreases in affinity and, in some cases, undetectable binding demonstrating the importance of sulfotyrosine recognition in chemokine signaling (12, 14–19).

While most chemokines form dimers or other oligomers, receptor activation is typically restricted to the monomeric ligand (20–24). However, structure-function studies of CXCL12 using preferentially monomeric ($CXCL12_{H25R}$) and constitutively dimeric ($CXCL12_2$) variants demonstrated that dimerization converts CXCL12 into a partial CXCR4 agonist that potently inhibits chemotaxis (25). As a CXCR4 ligand that stimulates intracellular calcium flux but fails to activate F-actin polymerization or β-arrestin recruitment, the $CXCL12_2$ dimer causes a type of ‘cellular idling’ that can block metastatic tumor formation in animal models for colorectal cancer and melanoma (26, 27). Differences in how the CXCR4 N-terminus is recognized by CXCL12 monomers and dimers may contribute to their distinct receptor activation profiles (26). For instance, in the NMR structure of the $CXCL12_2$:$CXCR4_{1–38}$ complex the receptor fragment wraps around both subunits of the CXCL12 dimer, placing sulfotyrosine 12 (sTyr12) and sTyr21 in distinct sites on one subunit while sTyr7 occupies a cleft at the dimer interface that would not exist in a CXCL12 monomer (25). In concordance with this structural model, it was observed that $CXCR4_{1–38}$ binding promotes CXCL12 dimerization (28). However, individual contributions of CXCR4 sulfotyrosines to the affinity and specificity of CXCL12 recognition and their impact on the monomer-dimer equilibrium remain unknown.

Site 1 contacts that contribute most to binding are potential targets for development of novel chemokine probes and antagonists. For example, we recently demonstrated that the sTyr21 binding pocket of CXCL12 can be targeted for inhibition by small molecule ligands that block CXCR4-mediated calcium signaling and chemotaxis (29, 30). This appears to be a conserved binding site, suggesting that sulfotyrosine-guided drug discovery may be a general strategy for targeting the chemokine family and other protein-protein interactions in the extracellular space (31).

Herein, a constitutively monomeric CXCL12 variant, termed $CXCL12_1$, was engineered to resist peptide-induced dimerization by maintaining steric repulsion of the chemokine helix. Six short CXCR4 peptides, centered on Tyr7, Tyr12, or Tyr21, were synthesized to study the contributions of individual sulfotyrosines in peptide binding and specificity. Peptides were titrated into $CXCL12_{WT}$, $CXCL12_2$, or $CXCL12_1$ and the interaction was monitored by 2D NMR. While sulfopeptides encompassing sTyr7 and sTyr12 interacted nonspecifically, an unsulfated Tyr7 peptide induced a new set of chemical shift

perturbations in the CXCL12 monomer that were also observed upon binding of the intact $CXCR4_{1–38}$ N-terminal domain. In contrast, the Tyr21 peptides bound specifically to the sTyr21 recognition site in all three CXCL12 variants, but exhibited a significantly higher affinity for $CXCL12_2$. The sTyr21 sulfopeptide correspondingly increased the CXCL12 dimerization affinity by eight-fold, revealing an allosteric coupling between the sulfotyrosine binding site and CXCL12 dimerization.

RESULTS AND DISCUSSION

Engineering a CXCL12 constitutive monomer

The monomer-dimer equilibrium complicates the structural analysis of CXCL12 interactions. A H25R substitution at the dimer interface discourages but does not prevent CXCL12 self-association (32), as binding of the CXCR4 N-terminus induces $CXCL12_{H25R}$ dimerization. In addition to Coulomb repulsion, a steric clash between the C-terminal α-helices of interacting CXCL12 monomers also limits dimer formation (33). The original NMR structure of $CXCL12_{WT}$ in acetate buffer (PDB ID 1SDF; (10)) possesses a helix orientation (~55° relative to the β-sheet) incompatible with dimerization. After analyzing the proximity and geometry of backbone and C^{β} atoms using the program Disulfide by Design (34), we constructed a disulfide-constrained CXCL12 monomer using L55C and I58C substitutions to limit helix rearrangement and prevent dimer formation (Fig. 1A). Non-reducing SDS-PAGE, 2D NMR and SEC-MALS analyses of $CXCL12_1$ demonstrate a properly folded, monomeric species (Supplemental Fig. 1). Whereas $CXCL12_{WT}$ self-associates with a K_d = 140 μM in 100 mM sodium phosphate (32), an HSQC dilution series of $CXCL12_1$ in the same conditions produced minimal chemical shift perturbations (Supplemental Fig. 1B). We concluded that the L55C/I58C disulfide stabilizes a monomeric CXCL12 conformation that is incompatible with dimer formation.

The CXCL12 monomer and dimer possess distinct $CXCR4_{1–38}$ binding sites

To establish a point of reference for subsequent measurements with smaller peptides, we monitored the binding of $CXCR4_{1–38}$ to the $CXCL12_1$ and $CXCL12_2$ variants by 2D NMR. Chemical shift mapping onto the $CXCL12_1$ model and $CXCL12_2$ NMR structure (Fig. 1B, C) highlighted perturbations across the β2 and β3 strands, consistent with the previous studies (25, 35), but $CXCL12_1$ also displayed additional contacts involving residues 58–61, 65, and 66 of the helix. Nonlinear fitting of chemical shift perturbations yielded K_d values of 3.5 ± 0.1 μM ($CXCL12_1$) and 0.9 ± 0.3 μM ($CXCL12_2$) (Fig. 1D). We recently demonstrated that perturbations induced by $CXCL12_{WT}$ binding to [*U*-^{15}N]-$CXCR4_{1–38}$ arise from the combination of distinct monomeric and dimeric interactions (26); in particular, CXCR4 residues 4–9 interact strongly with the preferentially monomeric $CXCL12_{H25R}$ variant but weakly with $CXCL12_2$. Taken together, these results suggest that the CXCR4 N-terminus makes unique contacts with the helix of monomeric CXCL12 that are occluded by dimerization of the chemokine.

CXCL12 binding of short CXCR4 sulfopeptides

Sulfation of the CXCR4 N-terminal extracellular domain at either Tyr21 alone or in combination with Tyr12 and Tyr7 enhances its affinity for CXCL12 (13). To assess the respective contribution of each sulfotyrosine, we synthesized short sulfated and unsulfated CXCR4 heptapeptides centered on each of the three tyrosine residues (Fig. 2A). Each peptide was acetylated and amidated to create uncharged N- and C-termini, respectively (36, 37). A total of six peptides were titrated into each CXCL12 variant and monitored by 2D ^{1}H-^{15}N HSQC experiments. For each titration, the chemical shift change of every residue was used to identify the binding site and calculate the interaction affinity. Table 1 contains a complete list of peptide binding affinities and binding energies.

As expected, the affinity of short CXCR4 peptides for all CXCL12 variants was greatly reduced relative to the intact $CXCR4_{1–38}$ N-terminal domain, with K_d values ranging from ~ 0.2–6 mM (Table 1). Interestingly, nearly all peptides bound most tightly to the $CXCL12_2$ locked dimer, whereas binding to $CXCL12_{WT}$ and $CXCL12_1$ were roughly equivalent. In titrations with each of the CXCL12 variants, chemical shift mapping indicated that peptides encompassing Tyr21 consistently bound to the previously defined sTyr21 pocket, as detailed below (Fig. 2D; Supplemental Fig. 2). In contrast, the Tyr7 and Tyr12 peptides did not localize to their corresponding interaction surfaces observed in the dimeric $CXCL12_2$:$CXCR4_{1–38}$ complex structure ((25); Fig. 2B,C). For example, in the NMR structure residues 4–10 of CXCR4 occupied a cleft at the dimer interface enabling sTyr7 to contact the R20 and V23 side chains of CXCL12. Here, the greatest shift perturbations (V49, T31 and F14) induced by the sTyr7 and sTyr12 sulfopeptides were more consistent with binding to the sTyr21 recognition site (Fig. 2; Supplemental Figs. 2 and 3).

Sulfopeptides bound with higher affinity than their unsulfated analogs, as observed in previous studies (13, 37, 38), with one notable exception. Binding of the unsulfated Tyr7 peptide to $CXCL12_1$ was roughly five-fold stronger than the sTyr7 sulfopeptide (Table 1). In contrast to the sTyr7 sulfopeptide, the unsulfated version induced substantial chemical shift changes in residues 23–25, 58–59, and 61 (Fig. 2E), matching the monomer-specific shift perturbations detected with $CXCR4_{1–38}$ (Fig. 1B). Titrations with $CXCL12_{WT}$ produced a similar pattern of shift perturbations and a twofold higher affinity for the unsulfated Tyr7 peptide (Supplemental Fig. 4), but there was no preferential binding to the $CXCL12_2$ dimer. Unlike Tyr21 which is rapidly modified by recombinant tyrosylprotein sulfotransferase-1 (TPST-1), Tyr7 sulfation is slow and not consistently predicted by the available algorithms (13). We postulate that contacts with the CXCR4 N-terminus are predominantly hydrophobic and favored when Tyr7 is unmodified and CXCL12 is monomeric.

The Tyr21 peptide exhibits high specificity and affinity

We monitored the binding of unsulfated $_{18}SGDYDSM_{24}$ and sulfated $_{18}SGDsYDSM_{24}$ to each CXCL12 variant by 2D NMR. Consistent with the $CXCL12_2$:$CXCR4_{1–38}$ complex structure, the unsulfated peptide produced chemical shift perturbations localized to residues in the β2 strand, β3 strand and N-loop of each variant (Fig. 3A; Supplemental Fig. 2). $CXCL12_{WT}$ and $CXCL12_1$ further exhibited shifts in residues 58 and 65–67 of the helix (Supplemental Fig. 2). Sulfation of Tyr21 strengthened the affinity of $_{18}SGDYDSM_{24}$ for all three CXCL12 variants and increased the magnitude of each perturbation without altering the pattern of responding residues (Table 1; Fig. 3B). The sTyr21 sulfopeptide bound to $CXCL12_2$ with the highest affinity (K_d = 211 μM) compared to all other peptide:chemokine combinations – four-fold stronger than the unsulfated variant (K_d = 831 μM).

Given that unsulfated $CXCR4_{1–38}$ (K_d = 0.9 μM) binds $CXCL12_2$ with a Gibbs free energy of −8.24 kcal mol^{-1}, our results suggest that the $_{18}SGDYDSM_{24}$ fragment alone provides about half of the binding energy ($\Delta G = -4.2$ kcal mol^{-1}) for the CXCR4:$CXCL12_2$ ‘site 1’ interaction. The identification of such hot spots, or regions of binding interfaces that contribute substantial binding energy, are of particular interest in the generation of protein-protein interface inhibitors (39). The major energetic contributions of the Tyr21 pocket justify our recent success in developing small molecules that antagonize receptor activation (29, 30). Further, identification of the hydrophobic Tyr7 pocket on monomeric CXCL12 demonstrates the utility of small receptor peptides in identifying druggable chemokine hot spots.

Tyr7 and Tyr12 are dispensable for CXCR4 activation by CXCL12

TPST enzymes catalyze the *O*-sulfation of Tyr21 much more efficiently than the Tyr12 or Tyr7 residues *in vitro* (28). Further, sTyr21 recognizes a cleft on CXCL12 that may be conserved across most members of the chemokine superfamily (25, 31). To test the hypothesis that Tyr21 sulfation is critical for receptor activation, tyrosine to alanine mutations were introduced into FLAG-tagged CXCR4 and expressed in CHO-K1 cells. CHO cells were chosen because they do not express endogenous CXCR4 and yield high levels of sulfated protein (40). Receptor activation was assessed by monitoring the calcium response as a function of increasing $CXCL12_{WT}$ concentrations (Fig. 3C). The response of CXCR4(Y7A) was similar to wildtype CXCR4 whereas the potency of CXCR4(Y12A) was reduced 3-fold. In contrast, CXCR4(Y21A) was significantly impaired both in terms of EC_{50} and efficacy. The combined mutation of Y7A, Y12A, and Y21A did not further diminish the potency relative to CXCR4(Y21A) but reduced the efficacy to ~20% of the wildtype receptor.

We hypothesize that protein misfolding is not responsible for the altered efficacies for two reasons. First, all of the mutants are surface-expressed at levels equivalent to the wildtype CXCR4 receptor (Supplemental Fig. 5). Second, the CXCR4 N-terminus is disordered and is not believed to participate in folding the overall tertiary structure of the receptor. This prompts the question of why there are efficacy changes at all. Our data suggests that the two-site model, in which site 1 is discretely responsible for chemokine binding and site 2 is specific for activation, is oversimplified and that both of these regions are ultimately required for full receptor activation. We conclude that sulfotyrosine modifications serve both to enhance CXCL12 binding affinity, and therefore potency, as well as signaling efficacy. Taken together, our results define the relative importance of individual CXCR4 sulfotyrosine modifications (Tyr21 > Tyr12 > Tyr7) for CXCL12 binding and receptor activation.

Binding at the Tyr21 site promotes dimerization

Chemokine dimerization is highly sensitive to numerous factors including GAGs, divalent anions, and pH (32). The CXCR4 N-terminus also promotes CXCL12 dimerization (28), which drastically alters the cellular response (25, 26). Interestingly, sTyr21 sulfopeptide binding to $CXCL12_2$ is 20-fold stronger than to $CXCL12_{WT}$ or $CXCL12_1$ (Fig. 3B). In addition, the sulfopeptide produces large perturbations at the dimer interface of $CXCL12_{WT}$ (Supplemental Fig. 2) suggesting it may allosterically induce $CXCL12_{WT}$ dimerization. We used intrinsic tryptophan fluorescence polarization (FP) to determine the K_d for $CXCL12_{WT}$ dimerization in the presence and absence of 3 mM sTyr21 sulfopeptide. The sulfopeptide shifts the K_d for $CXCL12_{WT}$ dimerization from 15.1 ± 0.4 mM to 2.6 ± 0.4 mM. Free sulfotyrosine (Tyr-SO_3H), which also binds the sTyr21 pocket (31), also promotes CXCL12 dimerization (K_d = 9.3 ± 1.8 mM; Fig. 4A).

The free energy changes derived from NMR binding (ΔG_{bind}) and FP dimerization (ΔG_{dimer}) measurements at 298 K were used to construct a thermodynamic cycle diagram (Fig. 4B). In pathway 1, CXCL12 binds the sTyr21 sulfopeptide (ΔG_{bind} = −3.8 kcal mol^{-1}) and then dimerizes (ΔG_{dimer} = −3.5 kcal mol^{-1}). When the sequence is reversed (pathway 2), CXCL12 dimerizes with ΔG_{dimer} = −2.5 kcal mol^{-1} and then binds the sTyr21 sulfopeptide with ΔG_{bind} = −5.0 kcal mol^{-1}. Analysis of both pathways yields similar coupling energies of −1.2 kcal mol^{-1} and −1.0 kcal mol^{-1}, respectively, that link CXCL12 dimerization to ligand binding in the sTyr21 recognition pocket. Similar studies with both CCL5 and CCL2 report binding of their respective N-terminal peptides, both sulfated and unsulfated, to promote dimer dissociation (38, 41). The apparent disparity between these studies and our data is most easily explained by the spatially distinct dimerization interfaces of CXC- and

CC-type chemokines. CXCL12 dimerizes through the β1 strand and α-helix whereas CC-type chemokines self-associates using the N-terminus, N-loop and β3 strand. Nonetheless, both chemokines bind sulfopeptides in the cleft formed by the N-loop and β3 strand. The close proximity of the sulfopeptide-binding site to the CC-type dimer interface is more consistent with dissociation through direct binding competition rather than an allosteric mechanism.

Conclusion

Many intracellular signal transduction complexes involve recognition of a recurring sequence motif by a protein interaction domain (42). Binding to certain short linear motifs (or SLiMs (43)) depends on post-translational modifications (PTMs) like phosphorylation, acetylation or methylation, and their corresponding recognition sites are often viewed as promising targets for drug discovery (44–46). Likewise, tyrosine sulfation enhances protein-protein interactions in the extracellular space (47), and sulfotyrosine recognition likely defines a new class of druggable extracellular targets (31). However, selective binding may require the combination of multiple SLiMs as observed for the WASP interacting protein (WIP) which uses three distinct recognition epitopes, including the conserved polyproline motif, to bind the EVH1 domain of N-WASP (48).

Many chemokine receptors contain multiple N-terminal tyrosines, which are predicted to be sulfated to different levels based on the suitability of the flanking sequences for TPST recognition (49, 50). We treated each tyrosine in the CXCR4 N-terminus as the center of a SLiM and found that the most efficient site of enzymatic sulfation (Tyr21) (13) is also the most important motif for binding to both CXCL12 monomers and dimers. Surprisingly, neither the Tyr7 or Tyr12 motif bound to a unique site on the CXCL12 dimer, and sulfation of the Tyr7 motif eliminated the site-specific binding to the CXCL12 monomer observed with the unsulfated Tyr7 motif. To our knowledge, this is the first demonstration that sulfation of chemokine receptors does not universally enhance complex affinity. In contrast, our data suggests that distinct patterns of tyrosine sulfation could encode selectivity either by enhancing or reducing affinity for unique recognition sites. Taken together this implies another layer of regulation for chemokine signaling. The structural basis for this effect awaits further study, but it appears that monosulfated (Tyr7/Tyr12/sTyr21) CXCR4 would exhibit a preference for the monomeric CXCL12 ligand while sulfation of Tyr7 would bias CXCR4 toward interactions with a CXCL12 dimer. Regardless, we conclude that the most functionally relevant mode of CXCL12-CXCR4 interaction involves specific recognition of a sulfotyrosine at position 21, and additional interactions with the receptor N-terminus that are independent of tyrosine sulfation.

Our results for CXCL12 binding to the sTyr21 motif in CXCR4 also suggest that chemokine oligomerization may be subject to allosteric control. Binding of the sTyr21 sulfopeptide, which is too short to contact both subunits of a CXCL12 dimer, significantly enhances CXCL12 dimerization by an indirect mechanism. Because dimerization converts CXCL12 into a partial agonist that potently inhibits chemotaxis and tumor metastasis (25–27), variations in the sulfation pattern of CXCR4 could in principle have functional consequences *in vivo*. Moreover, ligands that occupy the sTyr21 recognition site of CXCL12 may act as competitive inhibitors of receptor binding and allosteric modulators of chemokine function.

METHODS

Construction of $CXCL12_1$ plasmid

The $CXCL12_1$ variant was produced via mutagenesis of the $CXCL12_{WT}$ construct using complementary primers and the QuikChange Site-Directed Mutagenesis Kit (Stratagene) as per the manufacturer's instructions. The expression vector insert was confirmed by DNA sequencing.

Protein expression and purification

$CXCL12_{WT}$, $CXCL12_1$ and $CXCL12_2$ were expressed and purified as described previously (27). $CXCR4_{1–38}$, comprising the first 38 amino acids of CXCR4 preceded by a residual GlyMet dipeptide tag, was expressed and purified as previously described (28).

Size-exclusion chromatography multi-angle light scattering (SEC-MALS)

SEC was performed at a flow rate of 0.4 ml min^{-1} on a Superdex 75 10/300 GL analytical column (GE Healthcare) and monitored by an 18-angle MALS detector (Dawn Heleos II). $CXCL12_1$ (40 mg ml^{-1}; 5 mM) and $CXCL12_2$ (40 mg ml^{-1}; 2.5 mM) were solubilized in 25 mM MES (pH 6.8), 650 mM NaCl, and 0.02% (w/v) NaN_3. Samples were then applied to the column in a mobile phase of identical composition. Peak dispersion and average molar mass were calculated using Astra software.

NMR spectroscopy

All NMR spectra were acquired on a Bruker DRX 600 MHz spectrometer equipped with a ^1H, ^{15}N, ^{13}C TXI cryoprobe at 298 K. Experiments were performed with either 50 μM [*U*-^{15}N]-$CXCL12_{WT}$, -$CXCL12_1$, or -$CXCL12_2$ proteins in a solution containing 25 mM deuterated MES (pH 6.8), 10% (v/v) D_2O, and 0.02% (w/v) NaN_3. Full-length $CXCR4_{1–38}$ peptide titrations required 20 μM [*U*-^{15}N]-$CXCL12_1$ and -$CXCL12_2$ protein samples. Sulfated CXCR4 peptides were reconstituted at 100 mM in 25 mM deuterated MES, 10% (v/v) D_2O, and 0.02% (w/v) NaN_3 buffer. Unsulfated CXCR4 peptides were similarly reconstituted to 15 mM. Two separate $_4ISIYTSD_{10}$ peptide samples were reconstituted at 10 mM and 15 mM peptide in 25 mM deuterated MES, 10% (v/v) D_2O, 0.02% (w/v) NaN_3 buffer, from lyophilized powder. The 10 mM batch of $_4ISIYTSD_{10}$ peptide was titrated into $CXCL12_{WT}$ and $CXCL12_2$ and the 15 mM batch was titrated into $CXCL12_1$. $CXCL12_{WT}$ and $CXCL12_2$ chemical shift assignments (^1H and ^{15}N) were acquired from previously published sources (BMRB ID 16145 and 15633, respectively).

Peptides were titrated into CXCL12 samples and monitored by ^1H-^{15}N Heteronuclear Single Quantum Coherence (HSQC) experiments. Total peptide additions differed for individual peptide titrations but ranged from 0 – 160 equivalencies. Spectra were processed using in-house scripts and chemical shift tracking was performed using CARA software (51). Combined $^1H/^{15}N$ chemical shift perturbations were calculated as $((5\ \Delta\delta_H)^2+(\Delta\delta_{NH})^2)^{0.5}$, where δ_H and δ_{NH} are the amide proton and nitrogen chemical shifts, respectively. Equilibrium dissociation constants (K_d) were determined by nonlinear fitting of the combined $^1H/^{15}N_H$ chemical shift perturbations as a function of peptide concentration to a single-site quadratic equation (52). For a given interaction, residues with the largest chemical shift perturbations were fitted individually. The resulting K_d values and their respective fitting errors were then averaged to produce the reported affinity and standard deviation for that interaction.

Fluorescence polarization assay

Fluorescence polarization (FP) assays were performed on a PTI spectrofluorometer equipped with automated polarizers, using a time base polarization method provided by the program Felix32. Lyophilized $CXCL12_{WT}$ was reconstituted in H_2O and diluted to appropriate concentrations in a 25 mM MES (pH 6.8) buffer, filtered and degassed. $_{18}SGDsYDSM_{24}$ peptide and sulfotyrosine (Tyr-SO_3H) stocks were prepared separately at 25 mM and 500 mM, respectively, in a 25 mM MES (pH 6.8) buffer, filtered and degassed. Experiments were performed at 298 K and intrinsic tryptophan fluorescence was observed with emission and excitation wavelengths of 325 nm and 295 nm, respectively. FP was monitored as a function of increasing $CXCL12_{WT}$ concentration (10, 25, 50, 75, 100, 250, 500, 750, 1000 and 1500 μM) alone or in the presence of 3 mM $_{18}SGDsYDSM_{24}$ or 50 mM sulfotyrosine. The $CXCL12_{WT}$ dimerization equilibrium dissociation constant (K_d) was determined by non-linear fitting to a three-parameter function as previously described (32). Experiments were performed in duplicate and the reported dimerization K_d values reflect the average of both experiments.

Cell culture

Chinese hamster ovary K1 (CHO-K1) cells, stably transfected with the Gα15 gene in pcDNA3.1+, were cultured in a 1:1 mixture of Dulbecco's modified Eagle medium (DMEM) with Glutamax (Gibco):F12 nutrient mixture (Gibco) supplemented with 10% (w/v) fetal bovine serum (FBS) (Gibco). Stable expression of the Gα15 transgene was maintained by further supplementing the growth medium with 700 μg ml^{-1} geneticin (Gibco).

Transfections

For transient transfections with the Flag-CXCR4 WT and N-terminally mutated constructs, the CHO-K1 Gα15 stable cells were lifted using 0.25% (v/v) trypsin-EDTA (Gibco), and 2 × 10^6 cells were re-plated onto 10 cm culture dishes. To increase transfection efficiency, 0.25% (v/v) DMSO was added to the media when the cells were plated, and no geneticin was present in the plating medium. The cells were transfected 24 hours later using the Mirus TransIT-CHO Transfection Kit according to the manufacturers protocol, with the following exceptions: the amount of CHO transfection reagent was scaled up to 4 μl $μg^{-1}$ of DNA in the transfection mixtures, and the amount of CHO mojo reagent was scaled up to 1 μl $μg^{-1}$ of DNA in the mixtures. Immediately before transfection, the medium was replaced with a 1:1 mixture of DMEM with Glutamax:F12 nutrient mixture supplemented with 10% (w/v) FBS (without DMSO or geneticin).

Calcium flux

24 hours after plating, the medium was removed and the cells were washed with 5 ml PBS. The adherent cells were then incubated for 10 minutes in 3 ml of Cellstripper non-enzymatic cell dissociation solution (Cellgro). Cells were then suspended by pipetting, washed twice in Calcium Flux Buffer (Hanks Balanced Salt Solution supplemented with 20 mM HEPES) supplemented with 0.1% (w/v) bovine serum antigen (BSA) and 4 mM probenecid (Invitrogen). Each washing was carried out by centrifuging the cells at 350 × g and then re-suspending in Calcium Flux Buffer. After washing, the cell concentrations were normalized between samples and the cells were plated at 2.5 × 10^5 cells/well in poly-D-lysine coated 96 well plates (Becton Dickinson Labware). FLIPR 4 Calcium Flux assay kit dye (Molecular Devices) was then added to each well, such that the ratio of dye to cell suspension was 1:1. The plates were then centrifuged for 3 minutes at 250 × g to ensure the cells settled onto the surface of the plates. The plated cells were incubated at 310 K for 90 min. Fluorescence was measured at 310 K using a FlexStation2 Microplate Reader with excitation and emission

wavelengths at 485 nm and 515 nm, respectively. After an 18 s baseline measurement, the indicated concentrations of CXCL12 were added and the resulting calcium response was measured for an additional 50 s. Fluorescence as a function of CXCL12 concentration was fitted to a four-parameter equation. Data are representative of two experiments each performed with three replicates. CXCR4 variants with EC_{50} or maximum calcium response values more than three standard deviations from the mean $CXCR4_{WT}$ quantities were deemed significant.

Flow cytometry

For testing receptor surface expression, 3×10^5 cells were set-aside during the calcium flux assay preparations. The cells were then washed twice with PBS containing 0.5% BSA (w/v) (FACS buffer). Staining was carried out in a 50X dilution of either anti-DDDDK or mouse IgG1 isotype control conjugated to SureLight APC (Columbia Biosciences) for 45 minutes on ice. Cells were then washed 3X in FACS buffer before analysis, which was carried out using a Guava bench top mini-flow cytometer.

Supplementary Material

Refer to Web version on PubMed Central for supplementary material.

Acknowledgments

The authors would like to thank F.C. Peterson for fruitful discussion and careful review of the manuscript as well as R.B. Hill for expertise in operating the SEC-MALS. This work was supported by a Postdoctoral Fellowship from the Medical College of Wisconsin Cancer Center (JJZ), National Institutes of Health grants R01AI058072 (BFV), R01GM097381 (BFV), R56AI063325 (BFV), U01GM094612 (TMH), R01GM081763 (TMH), Cellular and Molecular Pharmacology Training Grant T32GM007752 (BS) and an Individual Ruth L. Kirschstein National Research Service Award Postdoctoral Fellowship F32GM103005 (JJZ). This work was also supported by an Australian Research Council Discovery Project Grant (RJP) and an Australian Postgraduate Award (DT).

REFERENCES

1. Ma Q, Jones D, Borghesani PR, Segal RA, Nagasawa T, Kishimoto T, Bronson RT, Springer TA. Impaired B-lymphopoiesis, myelopoiesis, and derailed cerebellar neuron migration in CXCR4- and SDF-1-deficient mice. Proc. Natl. Acad. Sci. U. S. A. 1998; 95:9448–9453. [PubMed: 9689100]
2. Zou YR, Kottmann AH, Kuroda M, Taniuchi I, Littman DR. Function of the chemokine receptor CXCR4 in haematopoiesis and in cerebellar development. Nature. 1998; 393:595–599. [PubMed: 9634238]
3. Sierro F, Biben C, Martinez-Munoz L, Mellado M, Ransohoff RM, Li M, Woehl B, Leung H, Groom J, Batten M, Harvey RP, Martinez AC, Mackay CR, Mackay F. Disrupted cardiac development but normal hematopoiesis in mice deficient in the second CXCL12/SDF-1 receptor, CXCR7. Proc. Natl. Acad. Sci. U. S. A. 2007; 104:14759–14764. [PubMed: 17804806]
4. Burns JM, Summers BC, Wang Y, Melikian A, Berahovich R, Miao Z, Penfold ME, Sunshine MJ, Littman DR, Kuo CJ, Wei K, McMaster BE, Wright K, Howard MC, Schall TJ. A novel chemokine receptor for SDF-1 and I-TAC involved in cell survival, cell adhesion, and tumor development. J. Exp. Med. 2006; 203:2201–2213. [PubMed: 16940167]
5. Hu X, Dai S, Wu WJ, Tan W, Zhu X, Mu J, Guo Y, Bolli R, Rokosh G. Stromal cell derived factor-1 alpha confers protection against myocardial ischemia/reperfusion injury: role of the cardiac stromal cell derived factor-1 alpha CXCR4 axis. Circulation. 2007; 116:654–663. [PubMed: 17646584]
6. Saxena A, Fish JE, White MD, Yu S, Smyth JW, Shaw RM, DiMaio JM, Srivastava D. Stromal cell-derived factor-1alpha is cardioprotective after myocardial infarction. Circulation. 2008; 117:2224–2231. [PubMed: 18427137]

7. Proulx C, El-Helou V, Gosselin H, Clement R, Gillis MA, Villeneuve L, Calderone A. Antagonism of stromal cell-derived factor-1alpha reduces infarct size and improves ventricular function after myocardial infarction. Pfluegers Arch. 2007; 455:241–250. [PubMed: 17520275]

8. Endres MJ, Clapham PR, Marsh M, Ahuja M, Turner JD, McKnight A, Thomas JF, Stoebenau-Haggarty B, Choe S, Vance PJ, Wells TN, Power CA, Sutterwala SS, Doms RW, Landau NR, Hoxie JA. CD4-independent infection by HIV-2 is mediated by fusin/CXCR4. Cell. 1996; 87:745–756. [PubMed: 8929542]

9. Balkwill F. Cancer and the chemokine network. Nat. Rev. Cancer. 2004; 4:540–550. [PubMed: 15229479]

10. Crump MP, Gong JH, Loetscher P, Rajarathnam K, Amara A, Arenzana-Seisdedos F, Virelizier JL, Baggiolini M, Sykes BD, Clark-Lewis I. Solution structure and basis for functional activity of stromal cell-derived factor-1; dissociation of CXCR4 activation from binding and inhibition of HIV-1. EMBO J. 1997; 16:6996–7007. [PubMed: 9384579]

11. Kofuku Y, Yoshiura C, Ueda T, Terasawa H, Hirai T, Tominaga S, Hirose M, Maeda Y, Takahashi H, Terashima Y, Matsushima K, Shimada I. Structural basis of the interaction between chemokine stromal cell-derived factor-1/CXCL12 and its G-protein-coupled receptor CXCR4. J. Biol. Chem. 2009; 284:35240–35250. [PubMed: 19837984]

12. Farzan M, Babcock GJ, Vasilieva N, Wright PL, Kiprilov E, Mirzabekov T, Choe H. The role of post-translational modifications of the CXCR4 amino terminus in stromal-derived factor 1 alpha association and HIV-1 entry. J. Biol. Chem. 2002; 277:29484–29489. [PubMed: 12034737]

13. Seibert C, Veldkamp CT, Peterson FC, Chait BT, Volkman BF, Sakmar TP. Sequential tyrosine sulfation of CXCR4 by tyrosylprotein sulfotransferases. Biochemistry. 2008; 47:11251–11262. [PubMed: 18834145]

14. Farzan M, Mirzabekov T, Kolchinsky P, Wyatt R, Cayabyab M, Gerard NP, Gerard C, Sodroski J, Choe H. Tyrosine sulfation of the amino terminus of CCR5 facilitates HIV-1 entry. Cell. 1999; 96:667–676. [PubMed: 10089882]

15. Preobrazhensky AA, Dragan S, Kawano T, Gavrilin MA, Gulina IV, Chakravarty L, Kolattukudy PE. Monocyte chemotactic protein-1 receptor CCR2B is a glycoprotein that has tyrosine sulfation in a conserved extracellular N-terminal region. J. Immunol. 2000; 165:5295–5303. [PubMed: 11046064]

16. Bannert N, Craig S, Farzan M, Sogah D, Santo NV, Choe H, Sodroski J. Sialylated O-glycans and sulfated tyrosines in the NH2-terminal domain of CC chemokine receptor 5 contribute to high affinity binding of chemokines. J. Exp. Med. 2001; 194:1661–1673. [PubMed: 11733580]

17. Colvin RA, Campanella GS, Manice LA, Luster AD. CXCR3 requires tyrosine sulfation for ligand binding and a second extracellular loop arginine residue for ligand-induced chemotaxis. Mol. Cell. Biol. 2006; 26:5838–5849. [PubMed: 16847335]

18. Gutierrez J, Kremer L, Zaballos A, Goya I, Martinez AC, Marquez G. Analysis of post-translational CCR8 modifications and their influence on receptor activity. J. Biol. Chem. 2004; 279:14726–14733. [PubMed: 14736884]

19. Fong AM, Alam SM, Imai T, Haribabu B, Patel DD. CX3CR1 tyrosine sulfation enhances fractalkine-induced cell adhesion. J. Biol. Chem. 2002; 277:19418–19423. [PubMed: 11909868]

20. Rajarathnam K, Sykes BD, Kay CM, Dewald B, Geiser T, Baggiolini M, Clark-Lewis I. Neutrophil activation by monomeric interleukin-8. Science. 1994; 264:90–92. [PubMed: 8140420]

21. Paavola CD, Hemmerich S, Grunberger D, Polsky I, Bloom A, Freedman R, Mulkins M, Bhakta S, McCarley D, Wiesent L, Wong B, Jarnagin K, Handel TM. Monomeric monocyte chemoattractant protein-1 (MCP-1) binds and activates the MCP-1 receptor CCR2B. J. Biol. Chem. 1998; 273:33157–33165. [PubMed: 9837883]

22. Laurence JS, Blanpain C, Burgner JW, Parmentier M, LiWang PJ. CC chemokine MIP-1 beta can function as a monomer and depends on Phe13 for receptor binding. Biochemistry. 2000; 39:3401–3409. [PubMed: 10727234]

23. Proudfoot AE, Handel TM, Johnson Z, Lau EK, LiWang P, Clark-Lewis I, Borlat F, Wells TN, Kosco-Vilbois MH. Glycosaminoglycan binding and oligomerization are essential for the in vivo activity of certain chemokines. Proc. Natl. Acad. Sci. U. S. A. 2003; 100:1885–1890. [PubMed: 12571364]

24. Tan JH, Canals M, Ludeman JP, Wedderburn J, Boston C, Butler SJ, Carrick AM, Parody TR, Taleski D, Christopoulos A, Payne RJ, Stone MJ. Design and Receptor Interactions of Obligate Dimeric Mutant of Chemokine Monocyte Chemoattractant Protein-1 (MCP-1). J. Biol. Chem. 2012; 287:14692–14702. [PubMed: 22396538]
25. Veldkamp CT, Seibert C, Peterson FC, De la Cruz NB, Haugner JC 3rd, Basnet H, Sakmar TP, Volkman BF. Structural basis of CXCR4 sulfotyrosine recognition by the chemokine SDF-1/CXCL12. Sci. Signaling. 2008; 1:ra4.
26. Drury LJ, Ziarek JJ, Gravel S, Veldkamp CT, Takekoshi T, Hwang ST, Heveker N, Volkman BF, Dwinell MB. Monomeric and dimeric CXCL12 inhibit metastasis through distinct CXCR4 interactions and signaling pathways. Proc. Natl. Acad. Sci. U. S. A. 2011
27. Takekoshi T, Ziarek JJ, Volkman BF, Hwang ST. A Locked, Dimeric CXCL12 Variant Effectively Inhibits Pulmonary Metastasis of CXCR4-Expressing Melanoma Cells Due to Enhanced Serum Stability. Mol. Cancer Ther. 2012; 11:2516–2525. [PubMed: 22869557]
28. Veldkamp CT, Seibert C, Peterson FC, Sakmar TP, Volkman BF. Recognition of a CXCR4 sulfotyrosine by the chemokine stromal cell-derived factor-1alpha (SDF-1alpha/CXCL12). J. Mol. Biol. 2006; 359:1400–1409. [PubMed: 16725153]
29. Veldkamp CT, Ziarek JJ, Peterson FC, Chen Y, Volkman BF. Targeting SDF-1/CXCL12 with a ligand that prevents activation of CXCR4 through structure-based drug design. J. Am. Chem. Soc. 2010; 132:7242–7243. [PubMed: 20459090]
30. Ziarek JJ, Liu Y, Smith E, Zhang G, Peterson FC, Chen J, Yu Y, Chen Y, Volkman BF, Li R. Fragment-based Optimization of Small Molecule CXCL12 Inhibitors for Antagonizing the CXCL12/CXCR4 Interaction. Curr. Top. Med. Chem. 2013; 12:2727–2740. [PubMed: 23368099]
31. Ziarek JJ, Heroux MS, Veldkamp CT, Peterson FC, Volkman BF. Sulfotyrosine recognition as marker for druggable sites in the extracellular space. Int. J. Mol. Sci. 2011; 12:3740–3756. [PubMed: 21747703]
32. Veldkamp CT, Peterson FC, Pelzek AJ, Volkman BF. The monomer-dimer equilibrium of stromal cell-derived factor-1 (CXCL 12) is altered by pH, phosphate, sulfate, and heparin. Protein Sci. 2005; 14:1071–1081. [PubMed: 15741341]
33. Veldkamp CT, Ziarek JJ, Su J, Basnet H, Lennertz R, Weiner JJ, Peterson FC, Baker JE, Volkman BF. Monomeric structure of the cardioprotective chemokine SDF-1/CXCL12. Protein Sci. 2009; 18:1359–1369. [PubMed: 19551879]
34. Dombkowski AA. Disulfide by Design: a computational method for the rational design of disulfide bonds in proteins. Bioinformatics. 2003; 19:1852–1853. [PubMed: 14512360]
35. Gozansky EK, Louis JM, Caffrey M, Clore GM. Mapping the binding of the N-terminal extracellular tail of the CXCR4 receptor to stromal cell-derived factor-1alpha. J. Mol. Biol. 2005; 345:651–658. [PubMed: 15588815]
36. Simpson LS, Zhu JZ, Widlanski TS, Stone MJ. Regulation of chemokine recognition by site-specific tyrosine sulfation of receptor peptides. Chem. Biol. 2009; 16:153–161. [PubMed: 19246006]
37. Zhu JZ, Millard CJ, Ludeman JP, Simpson LS, Clayton DJ, Payne RJ, Widlanski TS, Stone MJ. Tyrosine sulfation influences the chemokine binding selectivity of peptides derived from chemokine receptor CCR3. Biochemistry. 2011; 50:1524–1534. [PubMed: 21235238]
38. Tan JH, Ludeman JP, Wedderburn J, Canals M, Hall P, Butler SJ, Taleski D, Christopoulos A, Hickey MJ, Payne RJ, Stone MJ. Tyrosine sulfation of chemokine receptor CCR2 enhances interactions with both monomeric and dimeric forms of the chemokine monocyte chemoattractant protein-1 (MCP-1). J. Biol. Chem. 2013; 288:10024–10034. [PubMed: 23408426]
39. Wells JA, McClendon CL. Reaching for high-hanging fruit in drug discovery at protein-protein interfaces. Nature. 2007; 450:1001–1009. [PubMed: 18075579]
40. Nielsen PF, Bak S, Vandahl B. Characterization of tyrosine sulphation in rFVIII (turoctocog alfa) expressed in CHO and HEK-293 cells. Haemophilia. 2012; 18:e397–e398. [PubMed: 22681385]
41. Duma L, Haussinger D, Rogowski M, Lusso P, Grzesiek S. Recognition of RANTES by extracellular parts of the CCR5 receptor. J. Mol. Biol. 2007; 365:1063–1075. [PubMed: 17101151]

42. Pawson T, Nash P. Assembly of cell regulatory systems through protein interaction domains. Science. 2003; 300:445–452. [PubMed: 12702867]
43. Edwards RJ, Davey NE, Shields DC. SLiMFinder: a probabilistic method for identifying over-represented, convergently evolved, short linear motifs in proteins. PLoS ONE. 2007; 2:e967. [PubMed: 17912346]
44. Machida K, Mayer BJ. The SH2 domain: versatile signaling module and pharmaceutical target. Biochim. Biophys. Acta. 2005; 1747:1–25. [PubMed: 15680235]
45. Vidler LR, Brown N, Knapp S, Hoelder S. Druggability analysis and structural classification of bromodomain acetyl-lysine binding sites. J. Med. Chem. 2012; 55:7346–7359. [PubMed: 22788793]
46. Herold JM, Ingerman LA, Gao C, Frye SV. Drug discovery toward antagonists of methyl-lysine binding proteins. Curr. Chem. Genomics. 2011; 5:51–61. [PubMed: 22145013]
47. Stone MJ, Chuang S, Hou X, Shoham M, Zhu JZ. Tyrosine sulfation: an increasingly recognised post-translational modification of secreted proteins. New Biotechnol. 2009; 25:299–317.
48. Peterson FC, Volkman BF. Diversity of polyproline recognition by EVH1 domains. Front. Biosci. 2009; 14:833–846.
49. Monigatti F, Gasteiger E, Bairoch A, Jung E. The Sulfinator: predicting tyrosine sulfation sites in protein sequences. Bioinformatics. 2002; 18:769–770. [PubMed: 12050077]
50. Liu J, Louie S, Hsu W, Yu KM, Nicholas HB Jr, Rosenquist GL. Tyrosine sulfation is prevalent in human chemokine receptors important in lung disease. Am. J. Respir. Cell Mol. Biol. 2008; 38:738–743. [PubMed: 18218997]
51. Keller, R. The Computer Aided Resonance Assignment/Tutorial. Zurich: CANTINA; 2004.
52. Ziarek JJ, Peterson FC, Lytle BL, Volkman BF. Binding site identification and structure determination of protein-ligand complexes by NMR a semiautomated approach. Methods Enzymol. 2011; 493:241–275. [PubMed: 21371594]

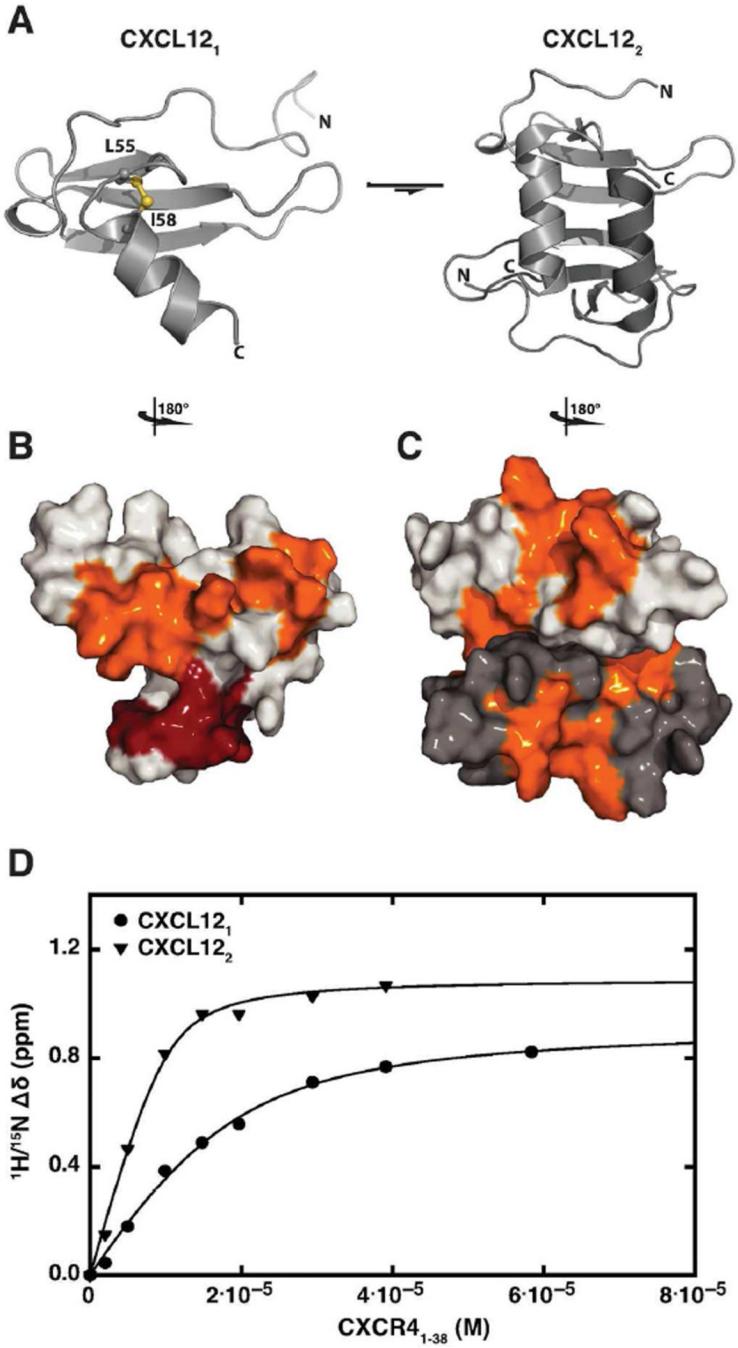

Figure 1. CXCL12$_1$ and CXCL12$_2$ have discrete CXCR4$_{1–38}$ binding sites

(A) The CXCL12 NMR structure (PDB ID 1SDF) solved in acetate (pH 4.9) was used to identify and model the I55C/L58C mutations for disulfide formation (yellow). Dimerization is inhibited when the helix is constrained to an acute angle relative to the β-sheet (33). Chemical shift perturbations (orange) produced by CXCR4$_{1–3}$ mapped onto **(B)** CXCL12$_1$ (PDB ID 1SDF) and **(C)** CXCL12$_2$ (PDB ID 2K01). Chemical shift perturbations unique to CXCL12$_1$ are highlighted in ruby. Both structures are rotated 180° relative to their respective ribbon representations. **(D)** CXCR4$_{1–38}$ induced chemical shift perturbations

fitted to a quadratic binding equation resulted in $CXCL12_1$ and $CXCL12_2$ affinities of 3.5 ± 0.1 and 0.9 ± 0.3 μM, respectively.

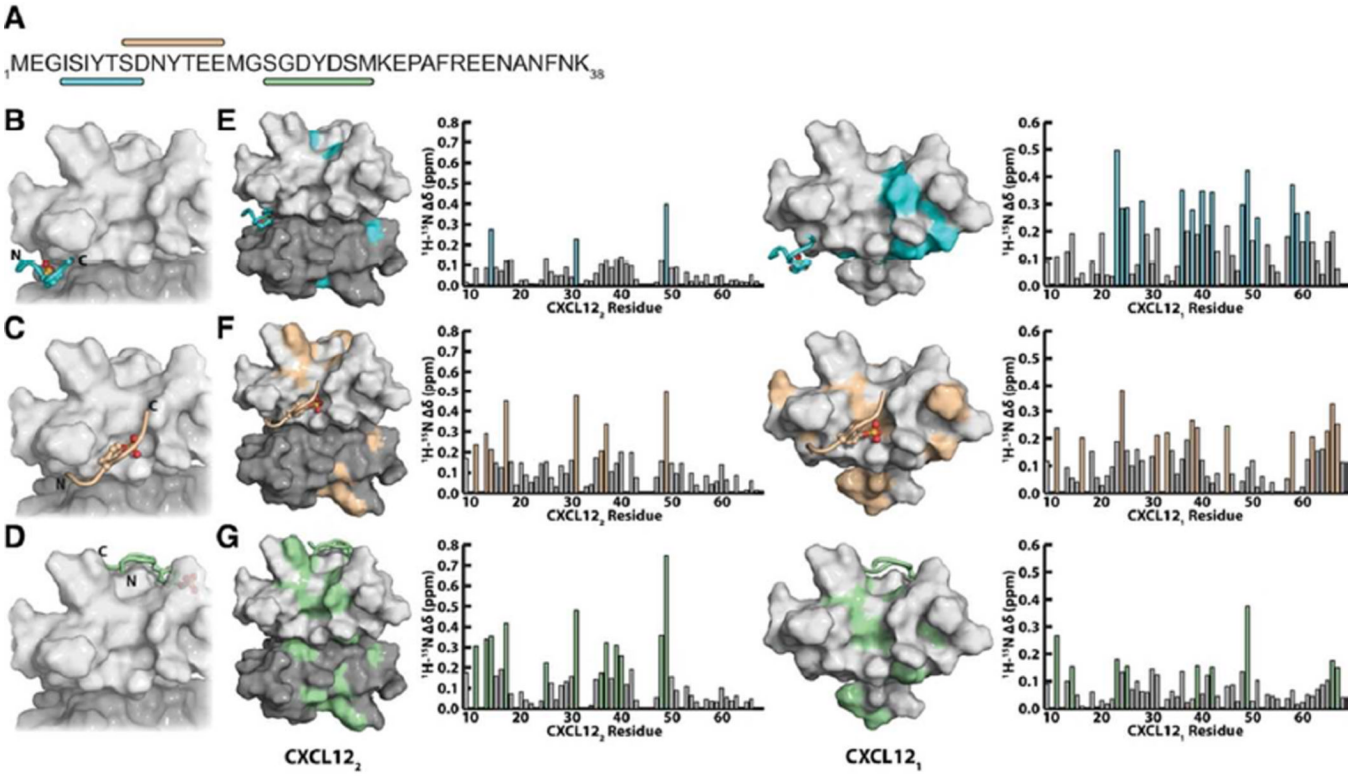

Figure 2. Chemical shift perturbations of CXCR4 sulfopeptides designed from the extracellular N-terminus

(A) The residues corresponding to the sTyr7 (cyan), sTyr12 (wheat), and sTyr21 (green) heptapeptides are indicated on the CXCR4 N-terminus amino acid sequence. The previously defined positions of sTyr7 (**B**), sTyr12 (**C**), and sTyr21 (**D**) heptapeptides are reproduced from the $CXCL12_2$:$CXCR4_{1–38}$ NMR structure (PDB ID 2K05). Chemical shift perturbations induced by sTyr7 (**E, left two panels**), sTyr12 (**F, left two panels**), and sTyr21 (**G, left two panels**) sulfopeptides map to the Tyr21 pocket on $CXCL12_2$ (PDB 2K05). In contrast, the chemical shift perturbations identify distinct binding sites for the sTyr7 (**E, right two panels**) and sTyr21 (**F, right two panels**) sulfopeptides on $CXCL12_1$ (PDB 2K05). Non-specific binding was observed for the sTyr12 sulfopeptide (**G, right two panels**).

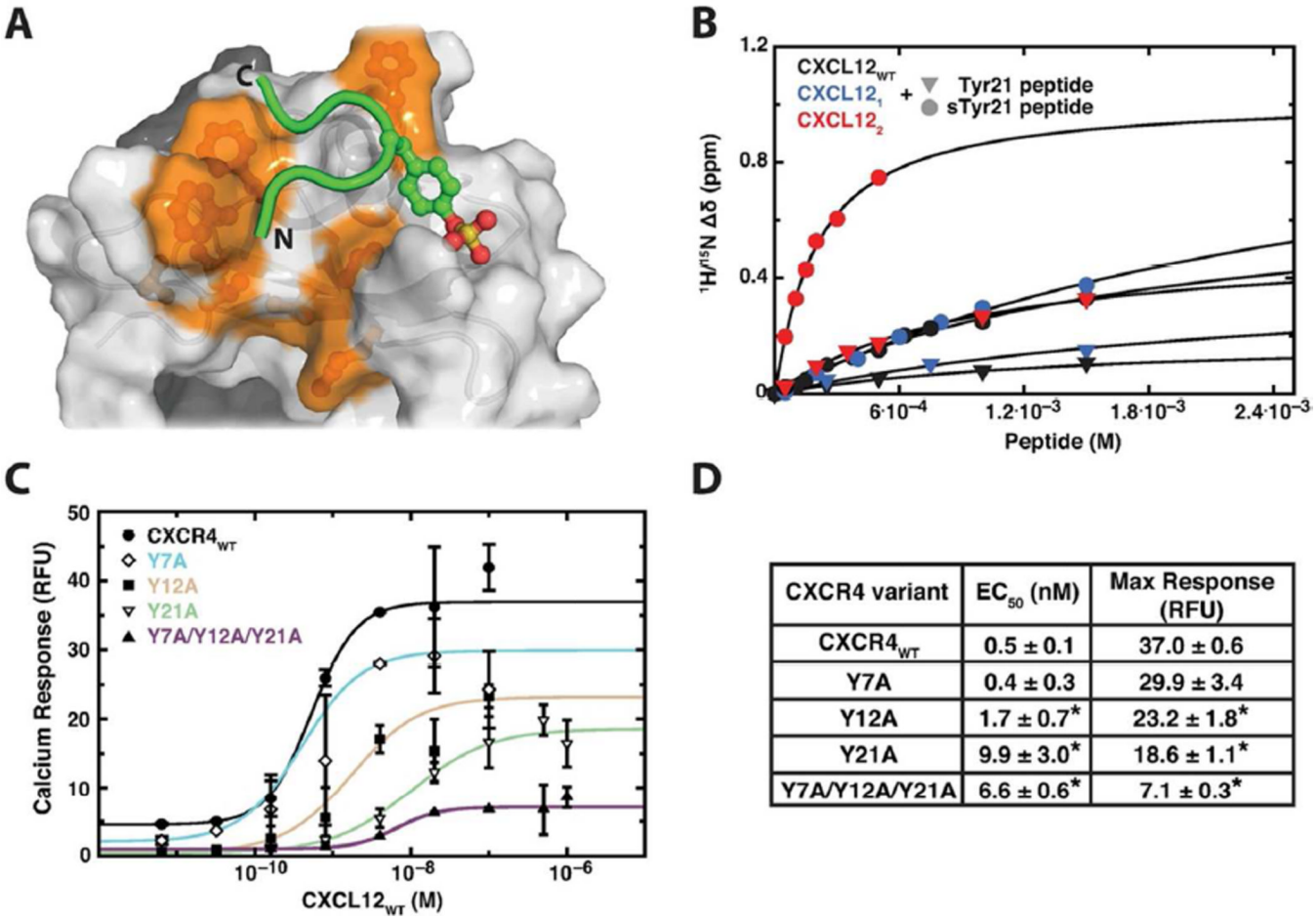

CXCR4 variant	EC_{50} (nM)	Max Response (RFU)
$CXCR4_{WT}$	0.5 ± 0.1	37.0 ± 0.6
Y7A	0.4 ± 0.3	29.9 ± 3.4
Y12A	1.7 ± 0.7*	23.2 ± 1.8*
Y21A	9.9 ± 3.0*	18.6 ± 1.1*
Y7A/Y12A/Y21A	6.6 ± 0.6*	7.1 ± 0.3*

Figure 3. Sulfation of Tyr21 improves sulfopeptide binding affinity and modulates full-length receptor activity

(A) The largest chemical shift perturbations (orange) are consistent with the putative sTyr21 sulfopeptide (green) binding site on $CXCL12_2$ (PDB ID 2K05). **(B)** Chemical shift perturbations induced by sulfated and unsulfated peptides were fitted to a quadratic binding equation to yield K_d values. The sTyr21 sulfopeptide (circles) bound $CXCL12_{WT}$ with K_d = 1.8 ± 0.2 mM (black), $CXCL12_1$ with K_d = 1.6 ± 0.2 mM (blue) and $CXCL12_2$ with K_d = 211 ± 23 μM (red). The Tyr21 peptide (triangles) bound $CXCL12_{WT}$ with K_d = 2.7 ± 0.5 mM (black), $CXCL12_1$ with K_d = 1.5 ± 0.4 mM (blue) and $CXCL12_2$ with K_d = 831 ± 137 μM (red). **(C)** The calcium response of FLAG-tagged CXCR4 variants was measured as a function of $CXCL12_{WT}$ concentration. Data are representative of two experiments each performed with three replicates. (**D**) Four parameter fits yielded each CXCR4 variants EC_{50} and maximum calcium response. CXCR4 variants with EC_{50} or maximum calcium response values more than three standard deviations from the mean $CXCR4_{WT}$ quantities are indicated with an asterisk.

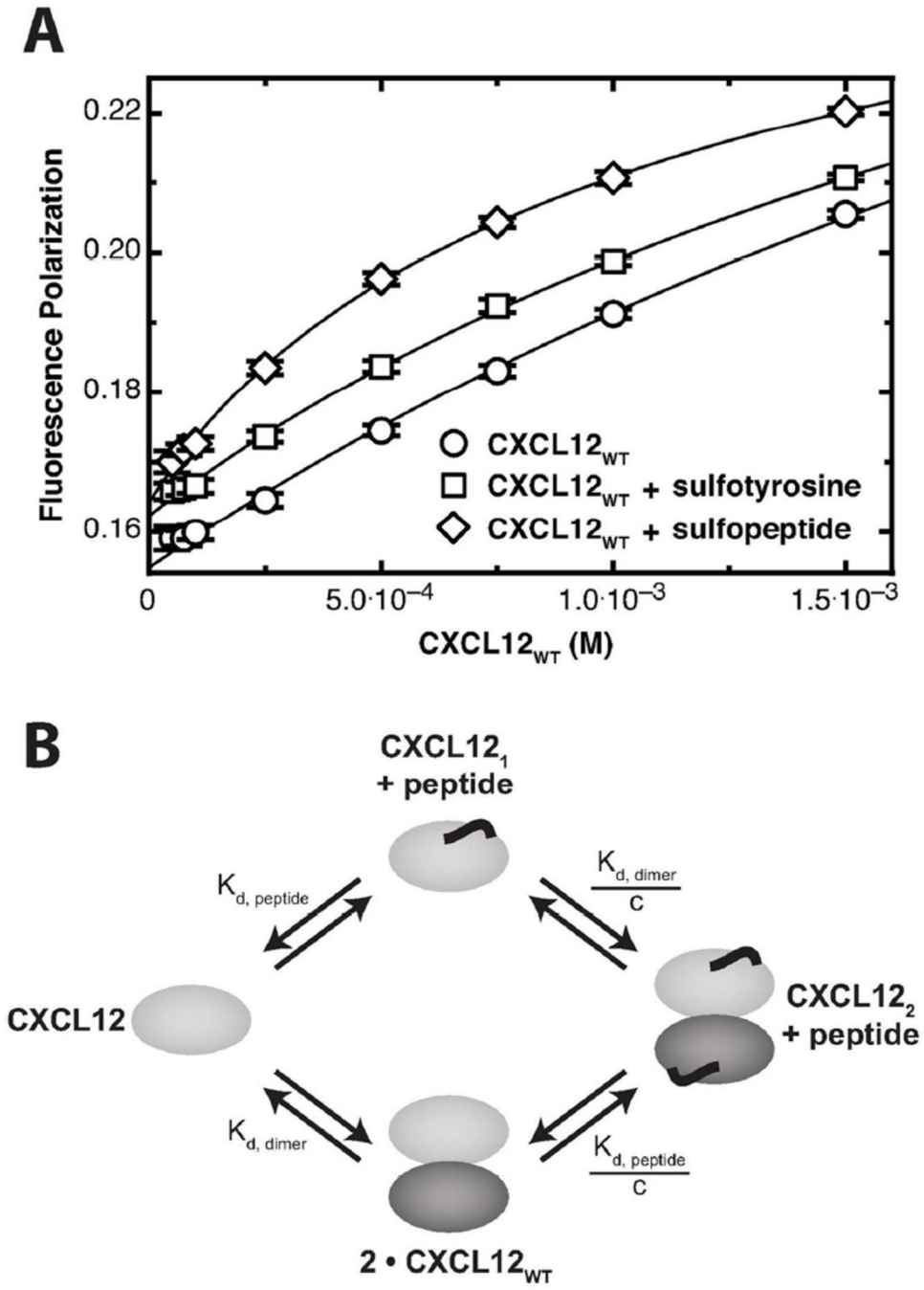

Figure 4. The sTyr21 binding site is allosterically linked to CXCL12 dimerization

(A) Intrinsic tryptophan fluorescence was used to calculate the $CXCL12_{WT}$ dimerization affinity alone (circles; K_d = 15.1 ± 0.4 mM), in the presence of 50 mM sulfotyrosine (squares; K_d = 8.9 ± 1.8 mM), or in the presence of 3 mM sTyr21 sulfopeptide (diamonds; K_d = 2.6 ± 0.4 mM). **(B)** FP and NMR derived binding affinities were used to produce a thermodynamic cycle, which illustrates that CXCL12 dimerization and sTyr21 sulfopeptide binding are coupled. After one ligand has bound, the affinity for the second ligand is enhanced with a cooperativity factor (c).

Table 1

Equilibrium dissociation constants and Gibbs' free energy of binding for peptide:CXCL12 variant complexes.

Peptide	$CXCL12_{WT}$		$CXCL12_1$		$CXCL12_2$	
	K_d	ΔG (kcal mol^{-1})	K_d	ΔG (kcal mol^{-1})	K_d	ΔG (kcal mol^{-1})
$CXCR4_{1–38}$	4.5 ± 2.2 μM *	−7.29 *	3.5 ± 0.1 μM	−7.43	0.9 ± 0.3 μM	−8.24
$_{18}$SGDsYDSM$_{24}$	1.8 ± 0.2 mM	−3.74	1.6 ± 0.2 mM	−3.81	211 ± 23 μM	−5.01
$_{18}$SGDYDSM$_{24}$	2.7 ± 0.5 mM	−3.50	1.5 ± 0.4 mM	−3.85	831 ± 137 μM	−4.20
$_{9}$SDNsYTEE$_{15}$	1.0 ± 0.1 mM	−4.09	1.8 ± 0.3 mM	−3.74	266 ± 38 μM	−4.87
$_{9}$SDNYTEE$_{15}$	2.1 ± 0.3 mM	−3.65	2.7 ± 0.8 mM	−3.50	332 ± 91 μM	−4.74
$_{4}$ISIsYTSD$_{10}$	4.3 ± 0.3 mM	−3.22	6.1 ± 1.3 mM	−3.02	386 ± 91 μM	−4.65
$_{4}$ISIYTSD$_{10}$	1.9 ± 0.3 mM	−3.71	1.1 ± 0.6 mM	−4.03	418 ± 60 μM	−4.60

$\Delta G = -RT \ln K_d$ @ 298 K

* K_d and ΔG calculated from Veldkamp et al. (32)

Non-specific binding to sY21 position